Copyright WILEY-VCH Verlag GmbH & Co. KGaA, 69469 Weinheim, Germany, 2018.

Supporting Information

Magnetic Living Hydrogels for Intestinal Localization, Retention and Diagnosis

Xinyue Liu, Yueying Yang, Maria Eugenia Inda, Shaoting Lin, Jingjing Wu, Yoonho Kim, Xiaoyu Chen, Dacheng Ma, Timothy K. Lu, and Xuanhe Zhao**

Calculation of the magnetic field

The magnetic field **B** around a disc-shaped magnet can be theoretically expressed as $\mathbf{B} = B_r\mathbf{e_r} + B_z\mathbf{e_z}$, where $\mathbf{e_r}$ and $\mathbf{e_z}$ are unit vectors in the direction of the positive *r*-axis and *z*-axis. B_r and B_z can be expressed written as[1]

$$B_r = -\frac{\mu_0}{4\pi} M \int_0^{2\pi}\int_0^a \left[-\frac{R(2r-2R\cos\Phi)}{2\left(R^2+(L/2-z)^2+r^2-2Rr\cos\Phi\right)^{3/2}} + \frac{R(2r-2R\cos\Phi)}{2\left(R^2+(L/2+z)^2+r^2-2Rr\cos\Phi\right)^{3/2}} \right] dRd\Phi \quad (1)$$

$$B_z = -\frac{\mu_0}{4\pi} M \int_0^{2\pi}\int_0^a \left[\frac{R(L/2-z)}{\left(R^2+(L/2-z)^2+r^2-2Rr\cos\Phi\right)^{3/2}} + \frac{R(L/2+z)}{\left(R^2+(L/2+z)^2+r^2-2Rr\cos\Phi\right)^{3/2}} \right] dRd\Phi \quad (2)$$

where (*r*, *z*) is the coordinate of the center of the magnetic hydrogel to the origin, μ_0 is the magnetic permeability in a classical vacuum, *M* is the scalar magnetization of the wearable magnet (the value ~ 1.14×10^6 A/m),[2] and *L* and *a* are the thickness and radius of the magnet, respectively.

Calculation of the intestinal propelling force

We started with the calculation of the intestinal propelling force F^{propel} which is equal to the intraluminal pressure p (i.e., the reported value ~ 6.6 kPa)[3] multiplied by the vertical cross-sectional area of the hydrogel, namely, $F^{\text{propel}} = 2pa_hL_h$, with a_h being the radius and L_h being the thickness of the disc-shaped hydrogel.

Calculation of the friction force

Given the normal force acting on the hydrogel $|F_z|$, we can further estimate the friction force as $F^{\text{friction}} = \mu|F_z|$, where $\mu = \beta(p_z)^{\alpha-1}$ is the frictional coefficient[4] with $\beta = 5.3$ and $\alpha = 0.54$ are parameters fitted by experimental data (**Figure S1g**) and $p_z = |F_z|/(\pi a_h^2)$ is the normal pressure.

Calculation of retained positions of magnetic hydrogels

We identified the physiological conditions and estimated the parameters for calculating the hydrogel retention in the mouse and human, including the dimensions of magnetic hydrogels (radius a_h = 1 mm for mouse and 10 mm for human, thickness L_h = 1 mm for both mouse and human), the magnetization of ingestible hydrogel (M_h = 60 kA/m, θ = 0, θ is the angle between M_h and the *z* axis), the friction coefficients between hydrogel and intestine under varied normal pressures (**Figure S1g**), and the distances between the intestine lumen and abdomen skin (D = 2 mm for mouse and 15 mm for human). The magnetic hydrogel's vertical position z_0 in the coordinate system is determined the distances between the wearable magnet and intestinal lumen, that is, $z_0 = L/2 + D$. To identify the horizontal position of retained magnetic hydrogels r_0, we plotted the net forces $(F^{\text{friction}} + F_r \cos\theta - F^{\text{propel}})$ in **Figure 2c, S9a,b, and S10a**. The magnetic hydrogel can be retained in the lumen if there are any locations at which net force is greater than or equal to zero, and the stably retained positions r_0 can be identified at which net force equals zero. Otherwise, the hydrogel passes through the tubular structure when the maximum net force is smaller than zero. We further calculated the normal pressures at the (r_0, z_0), that is, the retained positions or positions with the max net force (**Figure 2c,d and S9c,d**).

Analysis of magnetic retention in a mouse model

The retained magnetic hydrogel in a mouse model can impart a normal pressure as high as 5 kPa when the hydrogel is 2 mm away from a small magnet (a = 5.6 mm, L = 3.2 mm; **Figure S10b**), which is beyond the safe range for rodent intestinal tissues.[5] Considering the portable weight of the magnet (< 5% of mouse body weight; < 0.3% of human body weight), we further

identified the optimal magnet sizes, e.g., a = 25.4 mm, L = 12.7 mm for human and a = 5.6 mm, L = 1.6 mm for mouse intestinal retention (**Figure S4)**.

Safety of the extracorporeal magnet

We evaluated the effects of the magnetic field generated by the external magnet on both human body and external devices. As can be seen in **Figure S9e**, the magnitude of the magnetic field 5 mm away from the magnet (a = 25.4, L = 12.7 mm) was below the body exposure limit (400 mT) recommended by the International Commission on Non-Ionizing Radiation Protection (ICNIRP).[6] Attaching a layer of shielding material helped to reduce the magnitude of magnetic fields outside the body, thus minimizing the interference with some magnetic external devices, such as inductors, relays, and other magnets (**Figure S11**).[7]

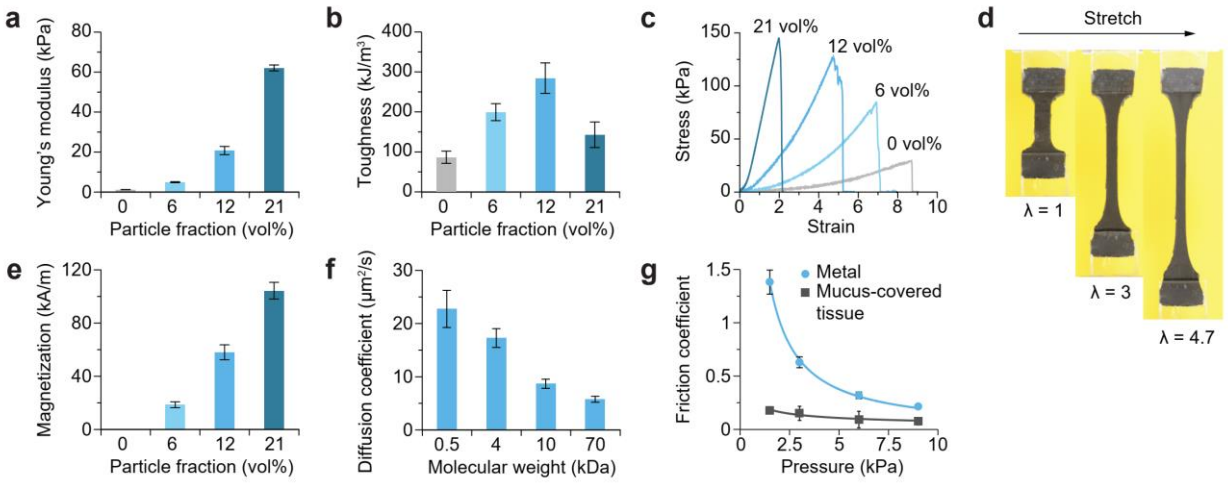

Figure S1. Characterization of the magnetic hydrogels. a) Young's modulus of the magnetic hydrogels at different particle concentrations. **b)** Toughness of the magnetic hydrogels at different particle concentrations. **c)** The stress-strain curves of the magnetic hydrogels at different particle concentrations. **d)** Photographs of the magnetic hydrogel (12 vol% NdFeB) at different stretches. λ, stretch. **e)** Magnitude of magnetization of the magnetic hydrogels at different particle concentrations. **f)** Diffusion coefficients of chemicals with varied molecular weights in the magnetic hydrogel (12 vol% NdFeB). **g)** Measured and fitted friction coefficients between the magnetic hydrogel (12 vol% NdFeB) and different substrates as a function of normal pressures.

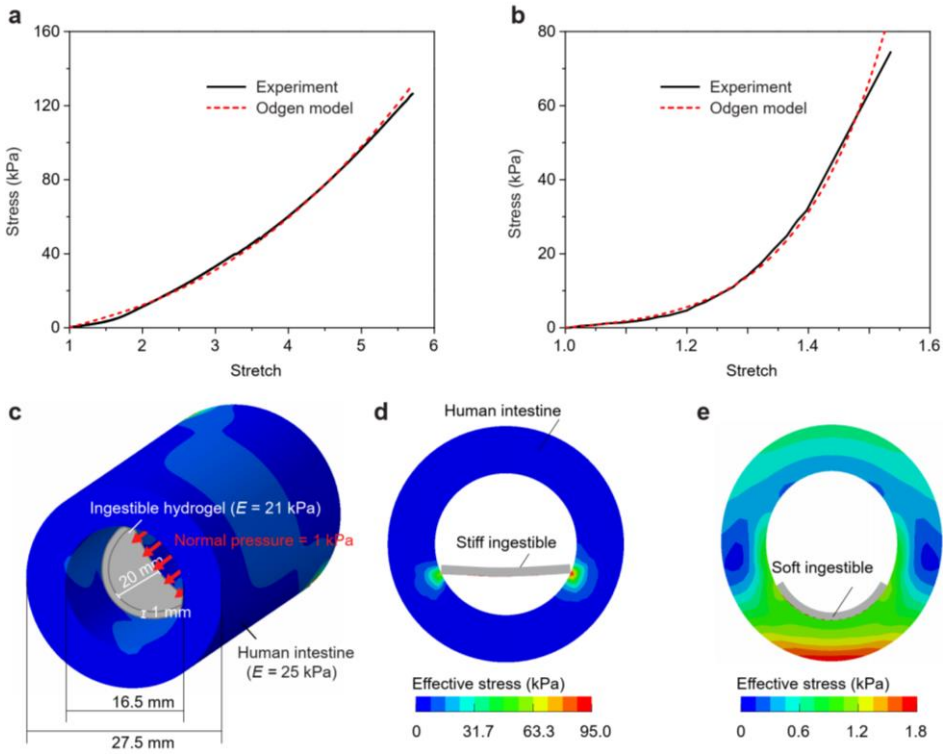

Figure S2. Finite element simulation of ingestible materials in the human intestine. a) Measured stress-strain curve and fitted curve using Odgen model for the magnetic hydrogel. **b)** Measured stress-strain curve and fitted curve using Odgen model for the intestinal tissue. **c)** Computer-aided engineering (CAE) model and dimensions used for finite element simulations of the human intestine contacting a disc-shaped ingestible hydrogel. **d-e)** Finite element simulations of disc-shaped ingestible materials (Young's modulus = 1 GPa in (**d)** and 21 kPa in **(e)**) contacting the human intestine when it is under the same normal pressure of 1 kPa.

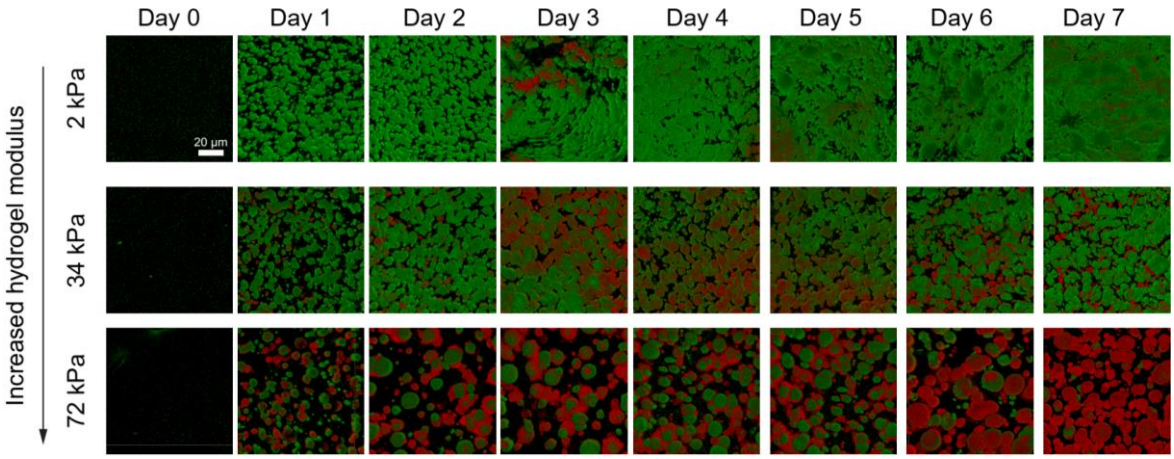

Figure S3. The effect of Young's moduli of magnetic hydrogels on bacterial viability. Encapsulation and live-dead assay of bacteria (*E. coli* DH5α) encapsulated in the magnetic hydrogels with different Young's moduli for 1–7 days. The encapsulated bacteria are stained with SYTO 9 dye (green) and propidium iodide (red) to visualize the viable and dead bacteria, respectively.

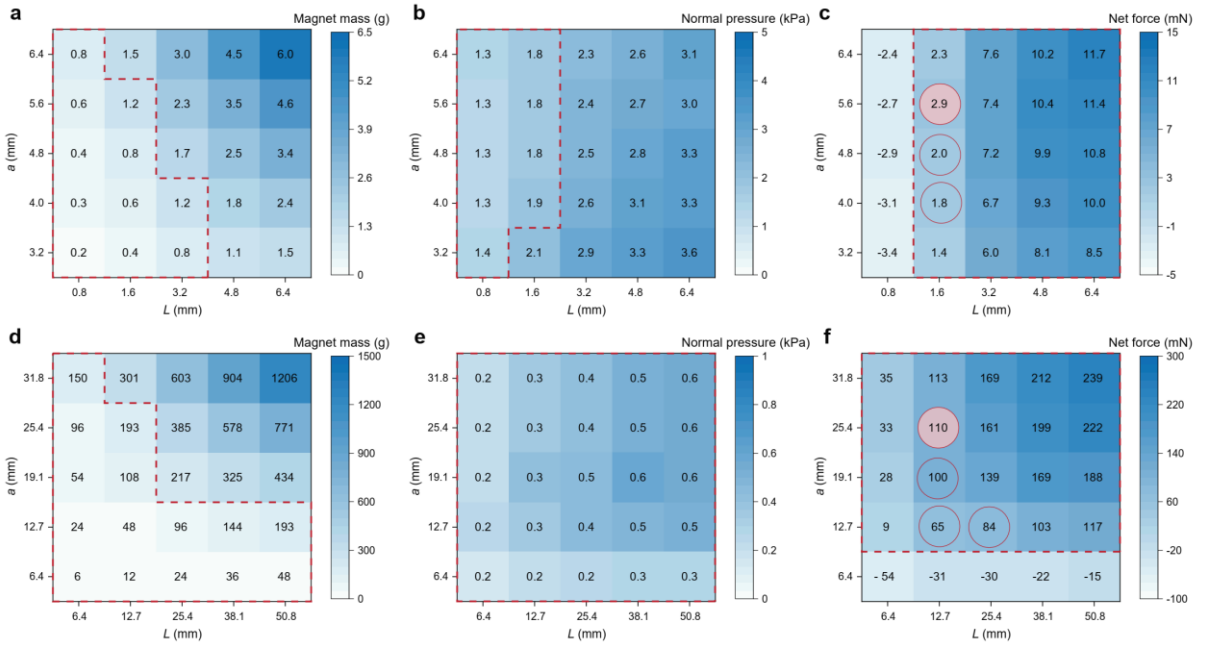

Figure S4. Magnet masses, normal pressures, and net forces for a range of magnet sizes. **a)** A heatmap of magnet masses for magnets attached to mice. The magnet masses less than 5% of mouse body weight (1.25 g) are highlighted with a red dashed border. **b)** A heatmap of average normal pressures applied by the magnetic hydrogels on the intestinal wall for magnets attached to mice. The average normal pressures less than 2 kPa are highlighted with a red dashed border. **c)** A heatmap of net forces ($F^{\text{friction}} + F_r \cos\theta - F^{\text{propel}}$) experienced by the magnetic hydrogel in mice. The net forces higher than 0 are highlighted with a red dashed border. Three magnets (open circles in **(c)**) satisfy the requirements of low magnet masses, low normal pressures, positive net forces, and commercial availability from K&J Magnetics. An optimal one (a solid circle in **(c)**) is chosen among them due to the highest net force. **d)** A heatmap of magnet masses for magnets attached to humans. The magnet masses less than 0.3% of human body weight (195 g) are highlighted with a red dashed border. **e)** A heatmap of average normal pressures applied by the magnetic hydrogels on the intestinal wall for magnets attached to humans. The average normal pressures less than 2 kPa are highlighted with a red dashed border. **f)** A heatmap of net forces ($F^{\text{friction}} + F_r \cos\theta - F^{\text{propel}}$) experienced by the magnetic hydrogel

in humans. The net forces higher than 0 are highlighted with a red dashed border. Four magnets (open circles in **(f)**) satisfy the requirements of low magnet masses, low normal pressures, positive net forces, and commercial availability from K&J Magnetics. An optimal one (a solid circle in **(f)**) is chosen among them due to the highest net force.

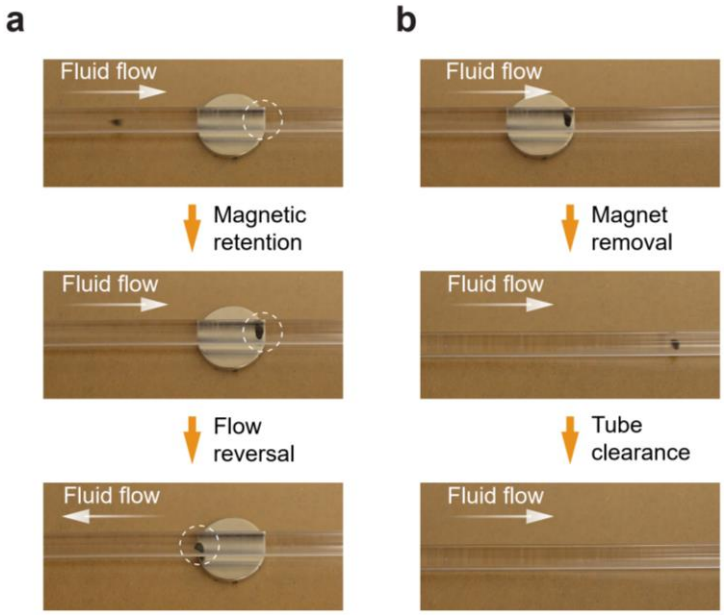

Figure S5. ***In vitro*** **magnet-assisted retention and release in a tube. a)** The retention of a magnetic hydrogel in a transparent plastic tube (diameter 2 mm) with an external magnet (radius 5.6 mm, thickness 1.6 mm) placed beneath the magnetic hydrogel. The magnetic hydrogel tends to cease at the downstream edge of the magnet. **b)** The release of a magnetic hydrogel in a transparent plastic tube. When the magnet is removed, the magnetic hydrogel resumes its mobility immediately and the tube is cleared.

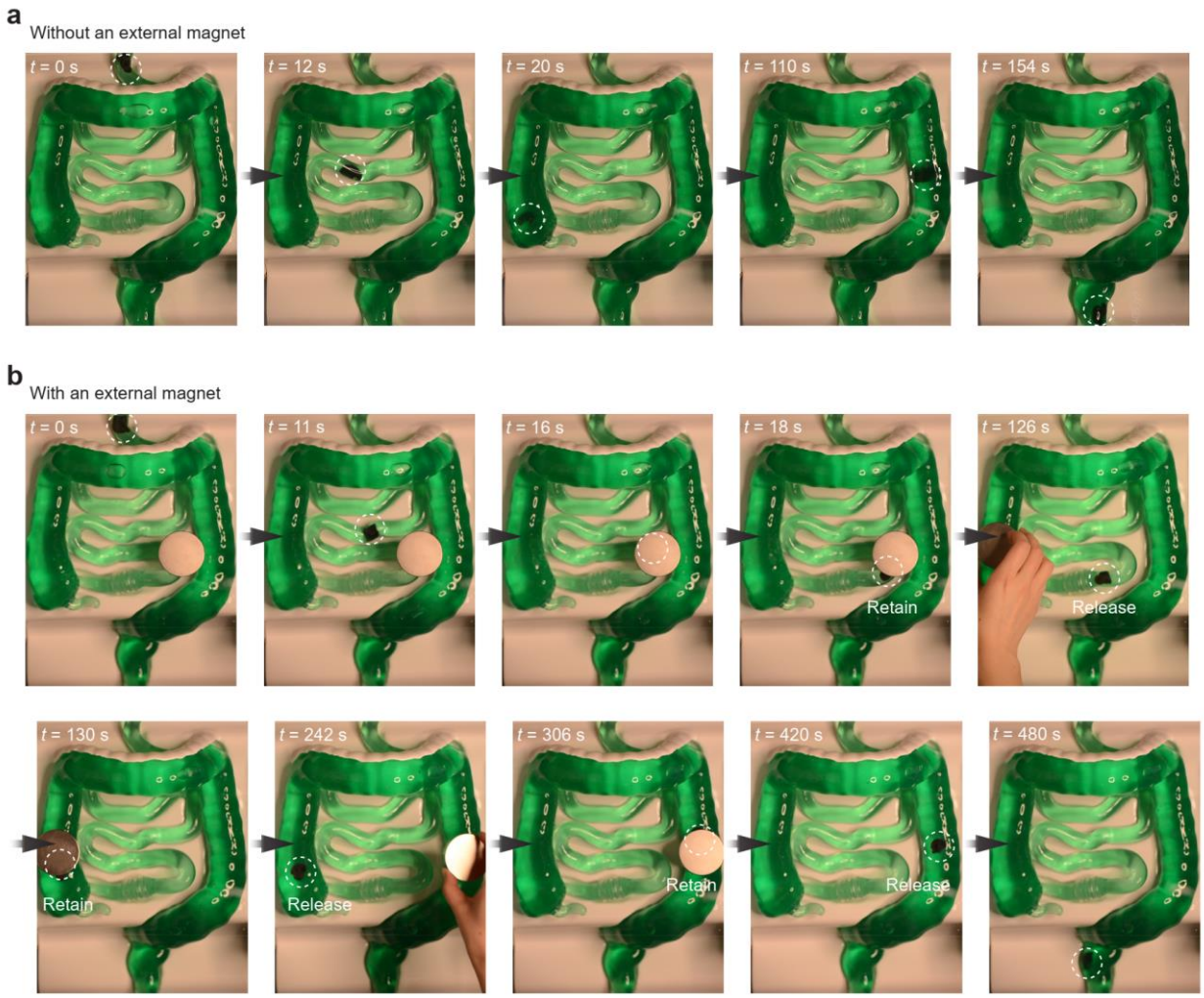

Figure S6. ***In vitro*** **magnet-assisted positioning in an intestinal phantom. a)** The magnetic hydrogel (not integrated with electronics) automatically passes through a silicone phantom without any navigation. **b)** If a magnet (radius 25.4 mm, thickness 12.7 mm) is placed on a transparent acrylic sheet right above the winding intestine phantom (distance 15–30 mm), the magnetic hydrogel is effectively pinned by the magnet at several different locations, such as small intestine, ascending colon, and descending colon for a long period of time (> 1 min).

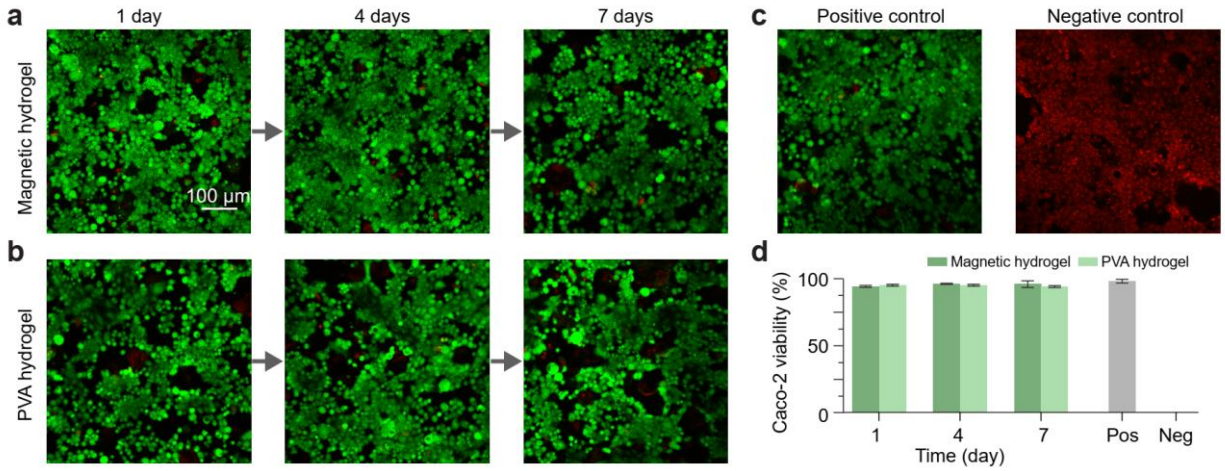

Figure S7. Biocompatibility of the magnetic hydrogel and PVA hydrogel. a) Live/dead assay of Caco-2 cells after a 2-day culture in a hydrogel-conditioned medium. To prepare the hydrogel-conditioned medium for live/dead assay, 20 mg of the magnetic hydrogel in 1 ml of DMEM at 37 °C for 1, 4, 7 days. **b)** Live/dead assay of Caco-2 cells after a 2-day culture in a hydrogel-conditioned medium. To prepare the hydrogel-conditioned medium for live/dead assay, 20 mg of the PVA hydrogel in 1 ml of DMEM at 37 °C for 1, 4, 7 days. **c)** Live/dead assay of positive and negative controls of Caco-2 cells. Cells without treatment and cells treated with 70% ethanol serve as positive and negative controls, respectively. The cells are stained with calcein (green) and ethidium homodimer-1 (red) to indicate the viable and dead ones, respectively. **d)** The Caco-2 cell viability calculated by the ratio of viable cells to all cells in the images. The values represent the mean ± s.d. (n = 3).

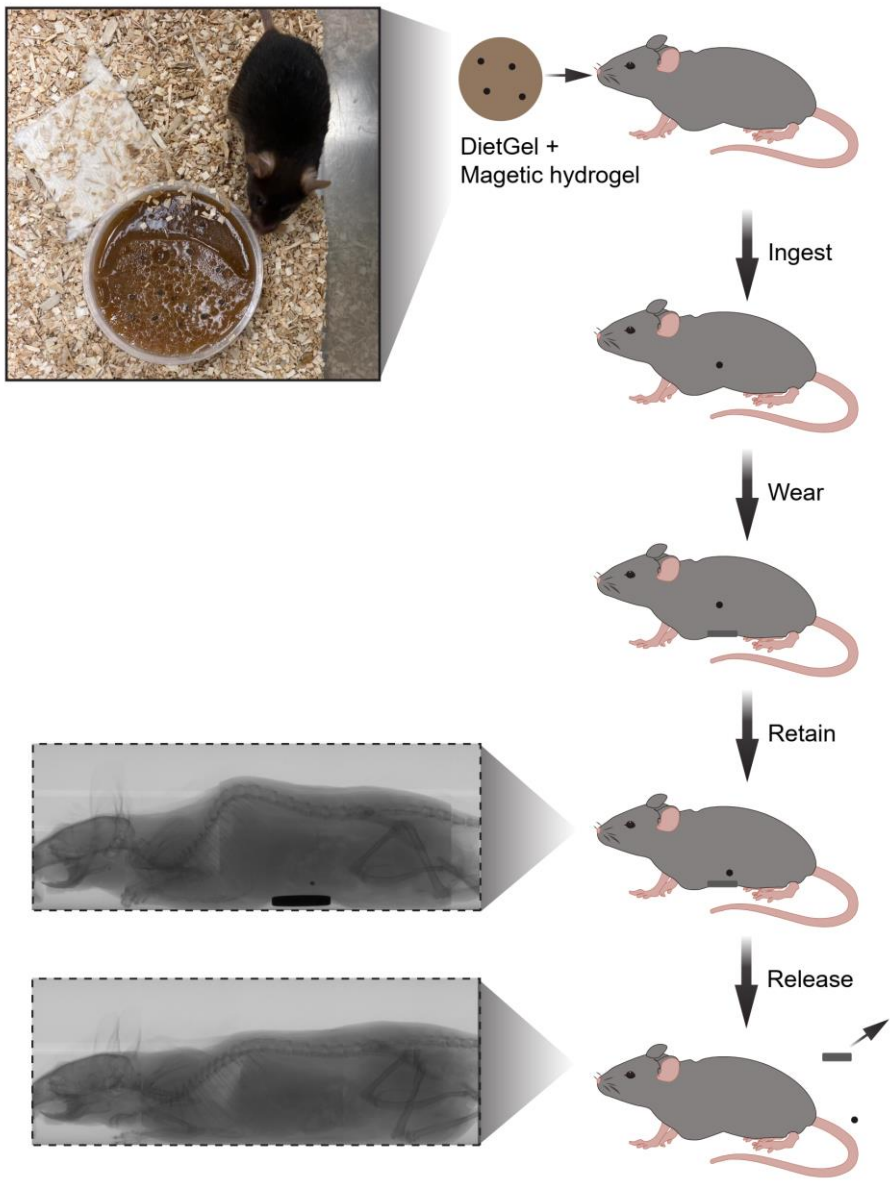

Figure S8. ***In vivo*** **procedures of magnet-assisted retention of the magnetic living hydrogels.** Magnetic hydrogels (radius 1 mm, thickness 1 mm) are dispersed in a block of nutritious jelly (DietGel 76A, ClearH_2O) and provided to mice after overnight fasting. When the hydrogels are ingested, the mice will wear a disc magnet on the abdomen skin to retain the hydrogel in the GI tract. After the removal of the magnet on the abdomen, the magnetic hydrogels get released rapidly and pass through the remaining tract.

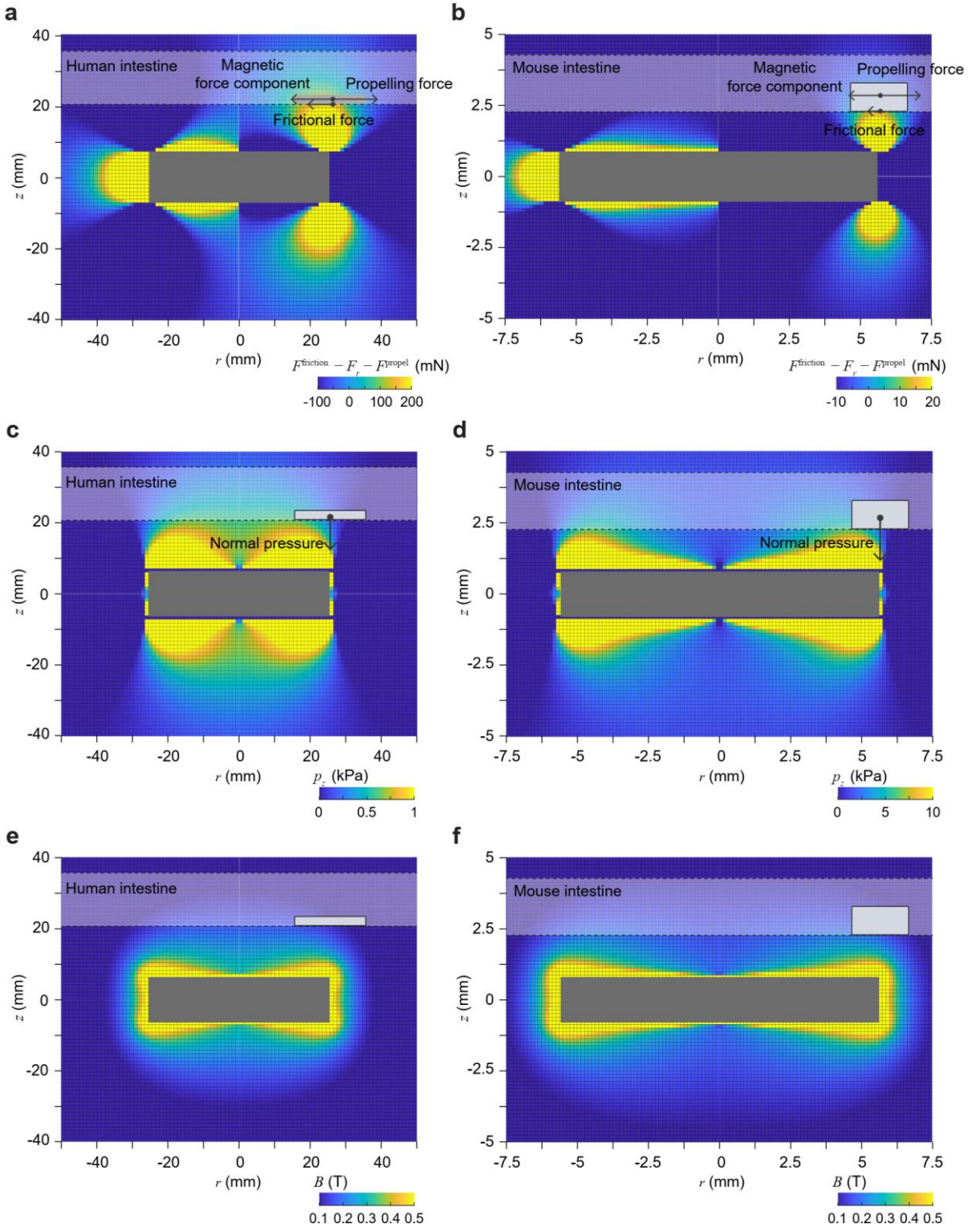

Figure S9. **Calculation of forces, normal pressures, and magnetic fields around an external magnet in a human and mouse model. a)** Net force $(F^{\text{friction}} + F_r \cos\theta - F^{\text{propel}})$ around a magnet (radius 25.4 mm, thickness 12.7 mm). **b)** Net force

$(F^{\text{friction}} + F_r \cos\theta - F^{\text{propel}})$ around a magnet (radius 5.6 mm, thickness of 1.6 mm). **c)** Normal pressure p_z applied by the magnetic hydrogel on the intestinal wall around a magnet (radius 25.4 mm, thickness 12.7 mm). **d)** Normal pressure p_z applied by the magnetic hydrogel on the intestinal wall around a magnet (radius 5.6 mm, thickness of 1.6 mm). **e)** Magnetic field (B, which is the scalar form of the magnetic field $B = |\mathbf{B}|$) calculated around a magnet (radius 25.4 mm, thickness 12.7 mm). **f)** Magnetic field (B) calculated around a magnet (radius 5.6 mm, thickness of 1.6 mm).

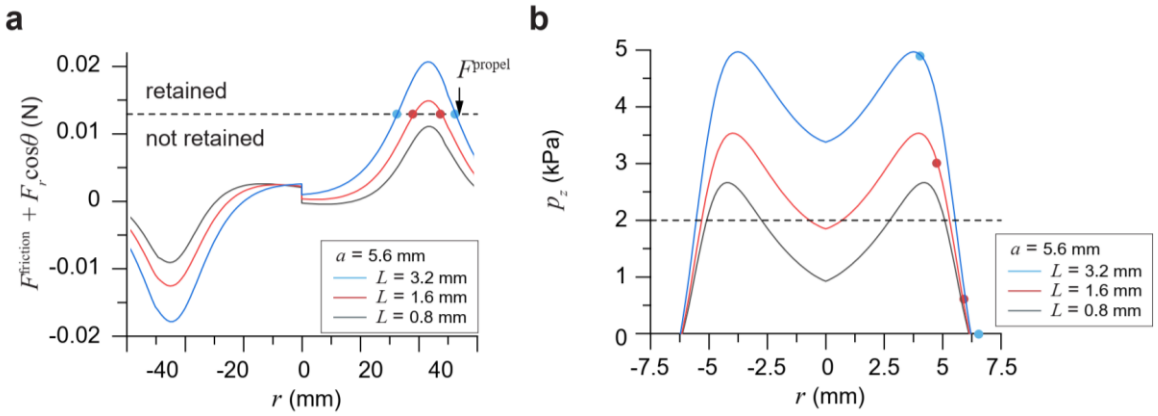

Figure S10. Model for intestinal retention and localization of the magnetic living hydrogels in the mouse model. a) Net retarding force $(F^{\text{friction}} + F_r \cos\theta)$ of a magnetic hydrogel (radius 1 mm, thickness 1 mm) at a vertical distance of 2 mm away from a magnet (radius 5.6 mm, thickness 0.8, 1.6, or 3.2 mm). The magnetic hydrogel can be retained when the net retarding force is higher than the propelling force F^{propel}. **b)** Normal pressure p_z applied by a magnetic hydrogel (radius 1 mm, thickness 1 mm) on the intestinal wall at a vertical distance of 2 mm away from a magnet (radius 5.6 mm, thickness 0.8, 1.6, or 3.2 mm). Solid circles on each curve in **(a)-(b)** indicate the stably retained locations for the magnetic hydrogel, in which the net retarding force $(F^{\text{friction}} + F_r \cos\theta)$ equals the propelling force F^{propel}.

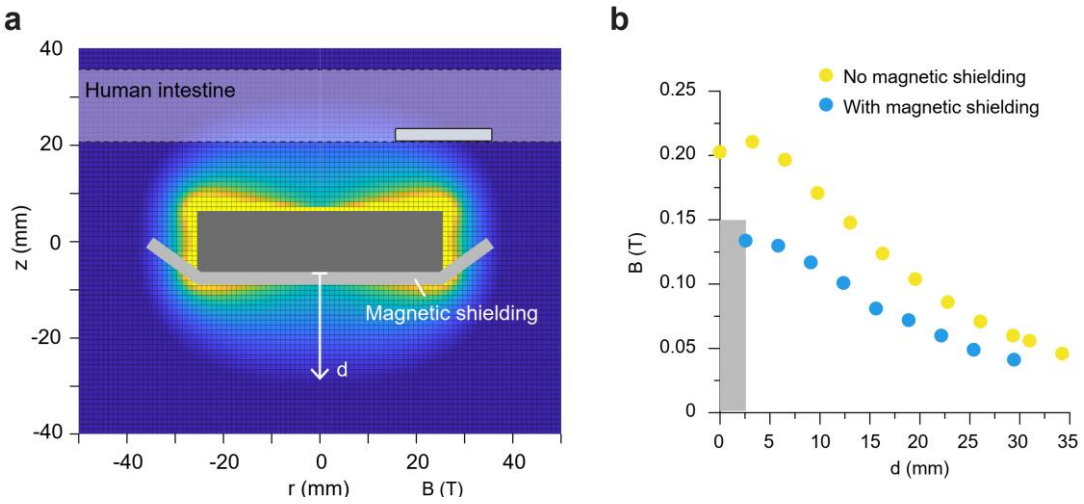

Figure S11. Effect of shielding materials on the magnetic field. a) Illustration of a sheet of magnetic shielding attached to the exterior surface of the wearable magnet. **b)** The magnetic field measured along the centerline of the magnet with and without a sheet of shielding material (thickness 2.6 mm) attached to the magnet. The peak of the magnetic field is decreased from 211 to 134 mT.

Supplementary Videos

Video S1. *In vitro* magnet-assisted retention and release in a tube. The retention of a magnetic hydrogel in a transparent plastic tube (diameter 2 mm) with an external magnet (radius 5.6 mm, thickness 1.6 mm) placed beneath the magnetic hydrogel. When the magnet is removed, the magnetic hydrogel resumes its mobility immediately and the tube is cleared.

Video S2. *In vitro* movement in an intestinal phantom without an external magnet. The magnetic hydrogel (not integrated with electronics) automatically passes through a silicone phantom without any navigation.

Video S3. *In vitro* positioning in an intestinal phantom with an external magnet. If a magnet (radius 25.4 mm, thickness 12.7 mm) is placed on a transparent acrylic sheet right above the winding intestine phantom (distance 15–30 mm), the magnetic hydrogel is effectively pinned by the magnet at several different locations, such as the small intestine, ascending colon, and descending colon for a long period of time (> 1 min).

Video S4. *In vivo* retention of the magnetic hydrogel in the mice intestine captured by microCT reconstruction. When an external magnet (radius 5.6 mm, thickness 1.6 mm) is attached on a mouse's abdomen, it can effectively pin the motion of magnetic hydrogels in the GI tract.

Video S5. *In vivo* movement of the magnetic hydrogel in the mice intestine captured by microCT reconstruction. Without an external magnet, the magnetic hydrogels move freely in the GI tract.

References

[1] S. M. Blinder, Magnetic Field of a Cylindrical Bar Magnet, http://demonstrations.wolfram.com/MagneticFieldOfACylindricalBarMagnet/, accessed.

[2] I. K&J Magnetics, Demagnetization (BH) Curves for Neodymium Magnets, https://www.kjmagnetics.com/bhcurves.asp, accessed.

[3] M. Hansen, *Physiological Research* **2002**, 51, 541.

[4] J. Gong, Y. Iwasaki, Y. Osada, K. Kurihara, Y. Hamai, *The Journal of Physical Chemistry B* **1999**, 103, 6001.

[5] B. Laulicht, N. J. Gidmark, A. Tripathi, E. Mathiowitz, *PNAS* **2011**, 108, 2252.

[6] I. C. o. N.-I. R. Protection, *Health Physics* **2009**, 96, 504.

[7] T. J. Sumner, J. M. Pendlebury, K. F. Smith, *Journal of Physics D: Applied Physics* **1987**, 20, 1095.